marginal OPs on XR to that on DTS using a compartmental approach. The study population was part of a larger study of random volunteers assessing the diagnostic performance of a novel X-ray device (DTS). All subjects (aged ≥40 years, with or without knee pain or knee OA) had both knees imaged by DTS, XR and 1.5T MRI. OPs were defined as WORMS grade ≥1 (scale 0-7) on MRI, and on plain PA semiflexed knee XR (using Synaflexer™ and DTS as OARSI grade ≥1 (scale 0-3). Knee pain was assessed using WOMAC score. We calculated the sensitivity and specificity for DTS and XR for detection of OPs, using MRI as the reference standard. Logistic regression was used to assess the association of pain with the presence of OPs in each compartment. Zero-inflated Poisson regression model with random effects was used to take the effect of clustering into account.

Results: Eighty knees (40 subjects) were imaged. The mean age of subjects was 57 (SD ±11) years, 30 (75%) were women, 35 (88%) were White and 31 (78%) had a body mass index ≥25 kg/m^2. Prevalence of OPs on MRI was 48 in lateral femoral, 39 in medial femoral, 45 in lateral tibial, 39 in medial tibial compartments. The sensitivity of DTS for OP detection was 0.98, 0.97, 1.00, and 1.00, respectively, and was superior to XR (0.73, 0.79, 0.87, and 0.90) in all compartments. DTS was significantly superior to XR in both femoral (p=0.0005 and 0.029) and lateral tibial compartments (p=0.026). Differences were not significant for specificity (DTS: 0.97, 0.98, 0.89, and 0.93; XR: 1.00, 1.00, 0.91, and 0.83). For DTS, association between pain and prevalent OPs was seen in all compartments (Odds ratio (OR)=4.4, 6.4, 4.2, and 5.7; all p<0.02), but OPs detected by XR appeared to be more strongly associated with pain in all compartments (OR=5.0, 8.4, 5.9, and 6.3; all p<0.004).

Table 1. Prevalence of marginal osteophytes detected by XR, DTS and MRI

Modality	Compartment	Knee					
		Left		Right		ALL	
		N	%	N	%	N	%
XR	Lateral femur	18	45	17	43	35	44
	Medial femur	18	45	13	33	41	39
	Lateral tibia	23	58	19	48	42	53
	Medial tibia	23	58	19	48	42	53
DTS	Lateral femur	24	60	24	60	48	60
	Medial femur	21	53	18	45	39	49
	Lateral tibia	25	63	24	60	49	61
	Medial tibia	22	55	20	50	42	53
MRI	Lateral femur	24	60	24	60	48	60
	Medial femur	21	53	18	45	39	49
	Lateral tibia	22	55	23	58	45	56
	Medial tibia	21	53	18	45	39	49

Table 2. Diagnostic performance of XR and DTS for detection of marginal osteophytes

Modality	Compartment	Sensitivity (%)	Specificity (%)	Accuracy (%)
XR	Lateral femur	73	100	79
	Medial femur	79	100	90
	Lateral tibia	87	91	89
	Medial tibia	90	83	86
DTS	Lateral femur	98*	97	98
	Medial femur	97*	98	98
	Lateral tibia	100*	89	95
	Medial tibia	100	93	96

Table 3. Relationship between marginal osteophytes and pain, tested by logistic regression analysis

Modality	Compartment	Odds Ratio	p-value
XR	Lateral femur	5.0	0.0037
	Medial femur	8.4	0.0005
	Lateral tibia	5.9	0.0019
	Medial tibia	6.3	0.0012
DTS	Lateral femur	4.4	0.0095
	Medial femur	6.4	0.0011
	Lateral tibia	4.2	0.011
	Medial tibia	5.7	0.0023

Conclusions: DTS offers higher sensitivity for detection of OPs in both femoral and lateral tibial compartments. OPs that DTS detects are associated with pain, but OPs that XR misses may be clinically less important. Digital tomosynthesis offers superior detection of osteophytes than plain X-rays, and thus may potentially be used to establish the radiographic diagnosis of OA in a clinical and research setting.

431

EXPERIMENTAL VALIDATION OF ^{99M}TC-NTP 15-5 AS A RADIOTRACER FOR VIVO ASSESSMENT OF OSTEOARTHRITIS IN NUCLEAR MEDICINE

E. Miot-Noirault[1], F. Cachin[1,2], A. Vidal[1], P. Auzeloux[1], S. Askienazy[3], M. Filaire[4], S. Boisgard[1,5], J.-M. Chezal[1]
[1]UMR 990 INSERM, Clermont Ferrand Cedex, France; [2]Nuclear Med., Jean Perrin Cancer Ctr., Clermont Ferrand, France; [3]Cyclopharma Laboratoires, Clermont Ferrand, France; [4]Anatomy, Med. Faculty, Clermont Ferrand, France; [5]Orthopaedic Dept., Gabriel Montpied Hosp., Clermont Ferrand, France

Purpose: When considering the pathophysiologic basis of the degenerative pathologies of cartilage, proteoglycans (PG) appear as one of the primary targets for both the diagnosis and the therapy. Our lab develops a "cartilage targeting strategy" for nuclear medicine applications with the ^{99m}Tc-NTP 15-5 radiotracer that selectively binds to cartilage PG *in vitro* and *in vivo*. The purpose of this presentation is to report preclinical data in favour of the clinical transfer of ^{99m}Tc-NTP 15-5 as a radiopharmaceutical for functional imaging of cartilage.

Methods: We have assessed the pertinence of ^{99m}Tc-NTP 15-5 radiotracer for *in vivo* scintigraphic imaging of cartilage in preclinical animal models: (i) healthy animals and several animal species, (ii) in meniscectomized (MNX) animals developing osteoarthritis (OA).

^{99m}Tc-NTP 15-5 monitoring of OA was performed at regular intervals over 6 months after unilateral medial meniscectomy. (Sham operated animals were also monitored in the same conditions). Tracer uptake was quantified *in vivo* using standardized region-of interest-method and expressed as uptake ratios (i.e. uptake of operated knee/uptake of contralateral knee). ^{99m}Tc-NTP 15-5 imaging was compared with bone scintigraphy. Moreover, ^{99m}Tc-NTP 15-5 uptake by human articular cartilage specimens was assessed after *ex vivo* incubation. For these experiments, 6 osteoarthritic tibial plateaux providing from prosthesis surgery and two femorotibial joints providing from anatomy laboratory were incubated with ^{99m}Tc-NTP 15-5 for 30 min or 2h. SPECT/CT imaging was then performed and tracer uptake quantified using based-region-growing SPECT/CT method. Results were expressed as % incubated dose (ID) and also as cartilage/bone uptake ratio

Results: In healthy animals and many animal species (i.e. rabbit, guinea pig, rat, mouse), a high and specific accumulation of ^{99m}Tc-NTP 15-5 was observed in cartilage (about 5.5±1.7% of Injected Dose/g of tissue at 15 min after iv injection). ^{99m}Tc-NTP 15-5 accumulation was demonstrated by whole knee autoradiography to be restrained to medial and lateral compartments of the joint, with a very low accumulation within bone and muscle (<0.1% ID/g).

In MNX animals, ^{99m}Tc-NTP 15-5 accumulation in cartilage within the operated joint was observed to change in the same animals as pathology progressed. Scintigraphic ratio time course evidenced (1) an initial "increased scintigraphic ratio phase" associated to an hypertrophic response of cartilage (2) a "decreased scintigraphic ratio phase" correlated with a decrease in proteoglycan content. No change in bone radiotracer uptake was observed throughout 6 months.

For experiments with human articular cartilage, analysis of SPECT/CT fused images evidenced selective and intense uptake of ^{99m}Tc-NTP 15-5 within cartilage, and a low accumulation within bone and soft tissues. Cartilage/ bone uptake ratios were 2.2±0.2. Interestingly, regions of OA specimens of decreased radiotracer accumulation on SPECT images were clearly colocalized with areas of cartilage defect, as visualised by CT.

Conclusions: These experimental results provided relevant key data in favour of the clinical transfer of ^{99m}Tc-NTP 15-5, as a radiopharmaceutical for an early specific diagnosis and staging of OA in nuclear medicine.

Grants: Fondation pour la recherche Medicale; Regional Innovation Fund (FRi2)/OSEO.

432

DISTRIBUTION OF BONE MARROW LESIONS IS CLOSELY RELATED TO DENUDED CARTILAGE IN OSTEOARTHRITIS SUBJECTS

M. Bowes[1], S. Mclure[2], C.B. Wolstenholme[1], S. Williams[2], G.R. Vincent[1], J.C. Waterton[3], R.A. Maciewicz[3], A.J. Holmes[3], P.G. Conaghan[1]
[1]Imorphics Ltd, Manchester, United Kingdom; [2]Univ. of Leeds, Leeds, United Kingdom; [3]AstraZeneca, Alderley Park, Macclesfield, United Kingdom

Purpose: The spatial distribution of bone marrow lesions (BML) may provide complimentary data to the existing semi-quantitative analysis and

increase our understanding of their importance in osteoarthritis (OA). This study compares the distribution of BMLs with the distribution of denuded bone in a group of OA subjects

Methods: 88 individuals were selected from the OAI progression groups 0.B.1 and 1.B.1. The subjects chosen had K-L scores of 2 or 3; medial JSN > lateral JSN, medial osteophytes and ≥1° of varus mal-alignment. OA related bone marrow lesions were defined as poorly delineated region of hyperintensity located in the subchondral bone, excluding the region adjacent to ligament attachment sites. TSE and DESS-we images were manually segmented using EndPoint software (Imorphics, Manchester, UK), with the segmenter blinded as to time point, but not to subject.

A method for measurement of cartilage thickness was adapted to measure the amount of BML adjacent to the bone surface. A statistical model of bone was fitted to each image, generating a set of anatomically corresponded points on the femur, tibia and patella. The amount of BML adjacent to each corresponded point is measured by taking a normal from each point 15mm into the bone and recording the number of BML voxels traversed by the normal. At each point on the surface this provides a measure of BML 'thickness' adjacent to that point. Cartilage thickness was calculated in the same way, using normals projecting out from the bone.

The association of BML and denudation was also measured semi-quantitatively using visualizations as shown in Figure 2. BMLs were scored as either overlapping or adjacent to denuded bone, or not.

The distribution of bone marrow lesions in this population shows a clear pattern (Figure 1). In the femur, BMLs are found predominantly in the patellofemoral joint both medially and laterally, and in the medial femoro-tibial joint. They are almost completely absent in the lateral femoro-tibial joint. In the tibia BMLs are primarily found in the medial tibial compartment. In the patella BMLs are found across the whole joint, with slightly greater density on the lateral facet.

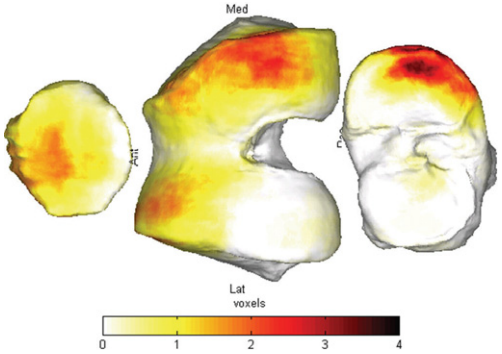

Figure 1. Distribution of BMLs in population. Figure shows average amount of bone marrow lesion across the surface of femur, tibia and patella. Scale is the mean number of BML voxels within 15 mm of the surface.

Table 1. Proportion of BMLs by compartment which overlap or are adjacent to areas of denuded cartilage

	All	Femur FP		Femur FT		Tibia		Patella	
		Med	Lat	Med	Lat	MT	LT	MP	LP
BMLs which overlap or are adjacent to denuded bobe	153	25	19	24	4	50	3	6	22
Total number of BML	199	28	27	37	7	53	7	10	30
(%)	(77)	(89)	(70)	(65)	(57)	(94)	(43)	(60)	(73)

In the baseline images 76.9% of all BMLs either overlapped or were adjacent to denuded bone (Table 1). Figure 2 shows the closeness of this relationship in 6 individuals whose pattern of denudation and BMLs was quite typical for this population. BMLs in the femoro-tibial joint and the lateral tibia overlapped less with denuded but were typically much smaller than those of the patellofemoral joint and patella. Separately we observed that there was no obvious correlation with BMLs and change in cartilage thickness (results not shown); in particular significant cartilage change was not seen in the patellofemoral joint of the femur, or in the patella.

Conclusions: A novel method of measurement and display of BMLs demonstrates that there is a striking similarity between the spatial distribution of BMLs and denuded bone in subjects with OA. Application of this method to compare BML with other outcomes may provide greater understanding of structural change in this disease

433

IMPROVEMENT OF THE REPRODUCIBILITY OF THE RADIOGRAPHIC KELLGREN-LAWRENCE (KL) SCORING SYSTEM IN HAND OSTEOARTHRITIS (HOA) USING A NEW KL SCORING SYSTEM AID

E. Maheu[1], P. Ravaud[2], G. Baron[2], F. Berenbaum[1], X. Chevalier[3], L. Gossec[4], D. Loeuille[5], J.-F. Maillefert[6], B. Mazières[7], F. Rannou[8], P. Richette[9], C. Cadet[10]

[1]St Antoine Hosp.-Rheumatology dept- AP-HP, Paris, France; [2]Biostatistics, Bichat Hosp-AP-HP, Paris, France; [3]Rheumatology, Henri Mondor hosp-AP-HP, Creteil, France; [4]Rheumatology B, Cochin Hosp- AP-HP, Paris, France; [5]Rheumatology, Vandoeuvre hosp., Vandoeuvre les Nancy, France; [6]Rheumatology, CHU Dijon, Dijon, France; [7]Rheumatology, CHU Larrey, Toulouse, France; [8]Reeducation dept, Cochin Hosp- AP-HP, Paris, France; [9]Rheumatology, Lariboisière hosp-AP-HP, Paris, France; [10]Rheumatology, Cabinet de rhumatologie, Paris, France

Purpose: KL is the most widely used radiographic scale to define HOA, assess HOA severity and follow-up radiographic progression. Though widely used for case-definition, its interobserver reliability is usually low in HOA.

Objectives: To study the impact of a new KL Scoring System Aid (KLSSA) on the reliability of KL scoring.

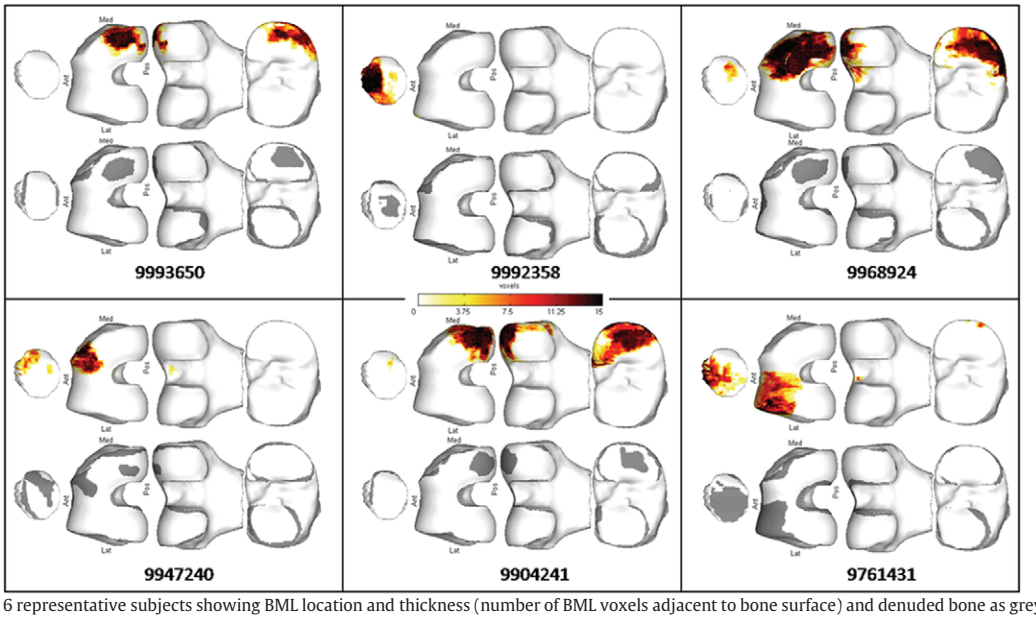

Abstract 432 – Figure 2. 6 representative subjects showing BML location and thickness (number of BML voxels adjacent to bone surface) and denuded bone as grey mask on the baseline image for each subject.